PCCP

Accepted Manuscript

This is an *Accepted Manuscript*, which has been through the Royal Society of Chemistry peer review process and has been accepted for publication.

Accepted Manuscripts are published online shortly after acceptance, before technical editing, formatting and proof reading. Using this free service, authors can make their results available to the community, in citable form, before we publish the edited article. We will replace this *Accepted Manuscript* with the edited and formatted *Advance Article* as soon as it is available.

You can find more information about *Accepted Manuscripts* in the Information for Authors.

Please note that technical editing may introduce minor changes to the text and/or graphics, which may alter content. The journal's standard Terms & Conditions and the Ethical guidelines still apply. In no event shall the Royal Society of Chemistry be held responsible for any errors or omissions in this *Accepted Manuscript* or any consequences arising from the use of any information it contains.

ROYAL SOCIETY OF CHEMISTRY

www.rsc.org/pccp

Cite this: DOI: 10.1039/c0xx00000x

www.rsc.org/xxxxxx

ARTICLE TYPE

Simultaneous SERS and surface-enhanced fluorescence from dye-embedded metal core-shell nanoparticles

Yan Zhou and Peng Zhang *

Received (in XXX, XXX) Xth XXXXXXXXX 20XX, Accepted Xth XXXXXXXXX 20XX

DOI: 10.1039/b000000x

We demonstrate a methodology to prepare Au-core/Ag-shell nanoparticles displaying both SERS and surface-enhanced fluorescence (SEF) activities simultaneously by embedding dye molecules between the core and the shell. Polyelectrolytes are used to adjust the spacing and the dye position between the core and the shell. Layer-by-layer polyelectrolyte deposition can serve as an effective and flexible way to introduce various types of dye molecules into the nanostructures. Results from the spectral measurements shed light to the intricacy between SERS and SEF.

Surface-enhanced Raman scattering (SERS) has been widely studied and applied for over three decades.[1] Raman scattering of molecules, despite being an inefficient process with very small cross-sections, can be greatly enhanced by orders of magnitude when the molecules reside in the vicinity of some metal nanostructures, those of silver and gold in particular.[2] It is generally agreed that SERS enhancement includes an electromagnetic field enhancement as the dominant contribution, and a chemical enhancement as the minor contribution.[3] The highly enhanced Raman signals have allowed SERS to become a useful tool in a number of studies.[4] Due to the inherently narrow and fingerprint-specific spectra, SERS offers a greater degree of multiplexing capability, as compared to the more widely used fluorescence-based detection schemes.[5]

Similar to the SERS effect, the fluorescence from a dye molecule may sometimes be increased when it is positioned near a metal nanostructure, a phenomenon known as surface-enhanced fluorescence (SEF).[6] It is considered that SEF is attributed by:[7] 1) enhanced absorption of light by the dye molecule due to the increased electromagnetic field around the metal nanoparticles; and 2) non-radiative coupling from the excited state of the dye molecule to the localized surface plasmon of the metal nanostructures, which is subsequently radiated by the nanostructures. Unlike SERS, a metal surface may either quench or enhance fluorescence of the nearby dye molecules. Early studies have indicated that a continuous transition from fluorescence quenching to fluorescence enhancement would occur as the metal-dye distance increases.[8] Yet it is still non-conclusive regarding the dye-metal distance where the metal would start to enhance the fluorescence, ranging from 10 nm to 1~2 nm.[7a,9]

Reports of simultaneous SEF and SERS observations are few and far between, partly because strong SERS usually occurs when the molecule and metal are very close, where fluorescence tends to be quenched.[10] Still, the combination of SEF and SERS onto single nanoparticles is highly desirable to improve the accuracy and sensitivity in detection applications, which has drawn increasing attention in recent years to study the two effects on the same nanostructures.[11] In this report, we demonstrate a methodology to prepare Au-core/Ag-shell nanoparticles displaying both SEF and SERS activities simultaneously by embedding dye molecules between the core and the shell. Polyelectrolytes deposited layer-by-layer onto the Au-core serve as the spacer to adjust the distance between the Au core and the Ag shell. By conjugating some polyelectrolytes with the dye molecules before assembling them layer-by-layer onto the gold core, the relative position of the dye molecules between the core and the shell can be controlled. The method is easy to implement, and can readily include a variety of dye molecules. We believe it is the first time such method is employed to realize SEF and SERS simultaneously on metal nanoparticles.

The general strategy of synthesizing the dye-embedded metal core-shell nanostructures is to coat the core nanoparticles with polyelectrolytes of alternate charges layer-by-layer before a final metal layer is deposited.[12] The two polyelectrolytes used in this study are polyacrylic acid (PAA) and polyallylamine hydrochloride (PAH), and the dye used is toluidine blue O (TBO). Some PAA polyelectrolytes are conjugated with TBO via the commonly used EDC-NHS method. Note that only a small fraction of the amino groups on PAA are labeled by the TBO molecules. AuNPs are first synthesized through thermal reduction of $HAuCl_4$ by citrate,[13] and washed thoroughly and redispersed in DI water. These AuNPs display negative surface charges. A layer of positively charged PAH is then adsorbed onto the AuNPs, followed by the adsorption of a negatively charged TBO-conjugated PAA layer. Hereafter, the layer assembly PAH-(PAA-TBO) is denoted as "1". Deposition of multiple polyelectrolyte layers is followed by alternating PAH and PAA adsorptions. Polyelectrolytes of lower molecular weights are chosen so that the polymer coils would not extend far beyond the Au core. Lastly, a silver shell is deposited on top of the polyelectrolytes to complete the TBO-embedded Au-core/Ag-shell nanostructure. The final nanoparticles are very stable and readily dispersible in water. All experimental details are provided in the supporting material. By substituting PAA-TBO for the different PAA layer, we can control the distance between the TBO molecules and the

Physical Chemistry Chemical Physics Accepted Manuscript

Au core, and that between TBO and the Ag shell. The thickness of the Ag shell can be adjusted by changing the amount of $AgNO_3$ solution used in the deposition of the Ag-shell. This scheme can be extended to embed other dye molecules, as long as they can be conjugated to one of the polyelectrolytes.

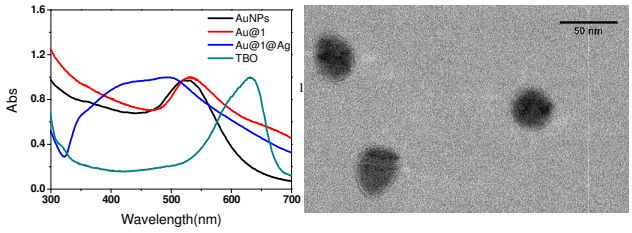

Figure 1. (Left) UV–vis spectra of AuNPs, Au@1, Au@1@Ag and TBO. (Right) TEM image of Au@1@Ag.

Figure 1 shows the UV-vis spectra and TEM image of the TBO-embedded Au-core/Ag-shell nanoparticles. The extinction spectrum of Au@1 includes the typical plasmon band of AuNPs (~520 nm) and the absorption band of TBO (~620 nm). The spectrum of Au@1@Ag contains a broad shoulder band at ~400 nm and a slightly blue-shifted AuNP plasmon band, both indicating the formation of the Ag-shell on the Au@1 nanoparticles. A distinct core-shell structure can be observed in the TEM image. The polyelectrolytes are too light to be seen in TEM, resulting in a small gap of 1~2 nm between the Au-core and Ag-shell. Collectively, these results suggest that, when $AgNO_3$ is reduced in the presence of Au@1 nanoparticles under the reaction conditions, Ag tend to deposit onto the surface of Au@1 instead of forming pure Ag nanoparticles in the solution.

Results from spectral measurements under 633 nm laser show that all samples of the TBO-embedded Au-core/Ag-shell nanoparticles exhibit strong and reproducible SEF and SERS signals simultaneously. Figure 2A shows the combined fluorescence and Raman spectra of Au@1 and Au@1@Ag. We are able to determine the enhancement factors (EFs) for both SEF and SERS of the dye molecules embedded in the Au-core/Ag-shell nanoparticles. Experimentally, this is done by removing the Au-core and Ag-shell of the TBO-embedded Au-core/Ag-shell nanoparticles with sodium cyanide (NaCN), and comparing the spectra of the sample before and after the treatment. Note that NaCN itself has little effect on the intensity of TBO fluorescence. The spectrum of the NaCN-treated sample is also shown in Figure 2A. Using the integrated intensity from 640 nm to 780 nm, we calculate the SEF EFs of Au@1 and Au@1@Ag to be 6.0 and 6.9, respectively. The results show that the Au core plays an important role on the fluorescence enhancement in both Au@1 and Au@1@Ag. In contrast, the Ag shell does not appear to enhance the fluorescence significantly. In some cases as shown in Figures 2B and 3C, the Ag shell actually quenches the fluorescence.

The EF estimation of SERS can be done similarly and as detailed in a previous study.[12] Because of the strong fluorescence of TBO under the 633 nm excitation, we used a 785 nm laser instead to determine the SERS EFs. Detailed information of SERS EF calculation is included in the supporting material. The SERS EFs of Au@1 and Au@1@Ag are calculated to be 8.3×10^3 and 3.0×10^5, respectively, under 785 nm excitation. While the Au-core is SERS-active, it is obvious that the presence of the Ag shell greatly enhances the SERS signals of the embedded TBO, as compared to the sample prior to the silver deposition. It should be emphasized that all fluorescence and Raman measurements in this study were done with liquid samples. Thus, the EFs (both SEF and SERS) in this report refer to the average values for the nanoparticles in the solution, and not that of individual nanoparticles. Note that, when depositing the polyelectrolytes (including the TBO-conjugated ones) onto the Au-core, the nanoparticles were thoroughly washed after each layer. There is little possibility of free TBO molecules adsorbed to any Ag nanoparticles that might be formed during the Ag-shell coating process.

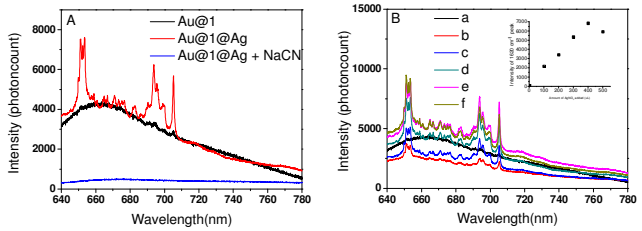

Figure 2. (A) SERS spectra of Au@1 and Au@1@Ag excited at 633 nm under the same conditions. (B) SERS spectra of Au@1@Ag prepared by adding different amounts of 1 mM $AgNO_3$ in the deposition step. a) 0 μL; b) 100 μL; c) 200 μL; d) 300 μL; e) 400 μL; f) 500 μL. Inset shows the SERS intensity of the 1620 cm^{-1} peak (at ~705 nm) vs. the amount of $AgNO_3$ added.

We have previously shown that SERS enhancement of reporters embedded in the Au-core/Ag-shell nanoparticles is very sensitive to the Ag shell thickness.[12] Here, we find that the same applies to the SEF enhancement. As shown in Figure 2B, the SEF and SERS enhancements are both affected by the Ag shell thickness. When Au@1 reacts with a small amount of $AgNO_3$, resulting in incomplete or very thin Ag shell, both the SEF and SERS signals of the embedded TBO are moderate. As the amount of $AgNO_3$ increases, both the SEF and SERS signal of TBO increases markedly, probably due to the formation of a complete Ag shell. Eventually, the SERS signals decrease when there is a fairly large amount of $AgNO_3$ added, probably because the Ag shell becomes too thick.

We have investigated the effect of the position of the TBO molecules between the core and the shell on their SEF and SERS EFs, by placing the embedded TBO in different electrolyte layers. Figure 3 shows the spectra of a number of different nanoparticles. These Au-core/Ag-shell nanoparticles, Au@1-$(PAH\text{-}PAA)_2$@Ag, Au@(PAH-PAA)-1-(PAH-PAA)@Ag and Au@$(PAH\text{-}PAA)_2$-1@Ag, have TBO embedded in the second, fourth and sixth layer, respectively. Their SEF and SERS spectra are similar in shape but with different intensities. The amount of TBO molecules in each nanoparticle is approximately the same, based on the similar fluorescence intensities of the NaCN-treated samples.

Physical Chemistry Chemical Physics Accepted Manuscript

This journal is © The Royal Society of Chemistry [year]

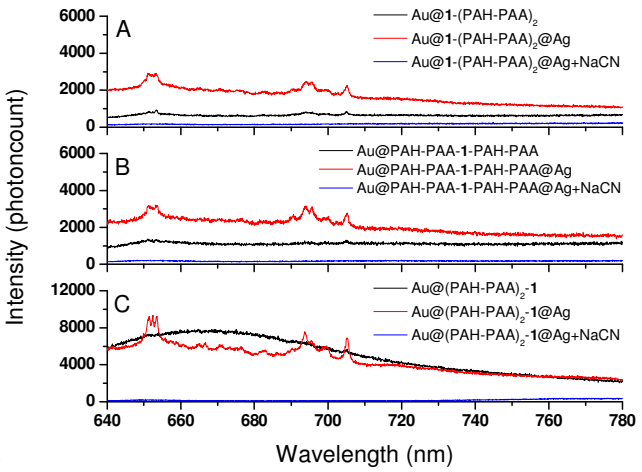

Figure 3. SERS spectra of three series of Au-core/Ag-shell nanoparticles, (A) Au@1-(PAH-PAA)$_2$@Ag, (B) Au@(PAH-PAA)-1-(PAH-PAA)@Ag, and (C) Au@(PAH-PAA)$_2$-1@Ag, respectively, collected under the same conditions.

Comparison among the three series of Au-core/Ag-shell nanoparticles leads to some interesting observations. In samples containing the Au core alone without the Ag shell, there is limited SERS enhancement. The closer the TBO molecules to the Au core, the higher the SERS EF. In samples containing both Au core and Ag shell, the distance between the embedded TBO molecules and the Ag shell plays an important role in the SERS enhancement. In particular, the Au@(PAH-PAA)$_2$-1@Ag nanoparticles display much higher SERS signals than the other two Au-core/Ag-shell nanoparticles. This is intriguing in that, while the whole volume between the Au core and Ag shell is a "hot zone" for SERS, the layer closest to the Ag-shell appears to experience the largest enhancement, probably because Ag is a better enhancer than Au.

The scenario is more complex for the SEF enhancement. The Au cores alone consistently enhance the fluorescence in Au@1-(PAH-PAA)$_2$, Au@(PAH-PAA)-1-(PAH-PAA) and Au@(PAH-PAA)$_2$-1 nanoparticles. As the distance between TBO and Au core increases, the SEF EF also increases. The SEF EFs of these Au-core nanoparticles are calculated to be 3.6, 6.4 and 25.6, respectively. The distances between the Au core and the TBO molecules in these nanoparticles are rather short, definitely less than 5 nm. The fact that they all display SEF could be due to: 1) the polyelectrolyte layer(s) may reduce the potential quenching by the Au core; and 2) the localized electromagnetic field is very strong.[14] Consider that SERS EFs are moderate for these Au-core nanoparticles, we suggest that the reduction in quenching by metal mostly account for the SEF in these nanoparticles. In contrast, while the Ag shell in Au@1-(PAH-PAA)$_2$@Ag and Au@(PAH-PAA)-1-(PAH-PAA)@Ag further enhances the fluorescence, it slightly quenches the fluorescence in Au@(PAH-PAA)$_2$-1@Ag. The SEF EFs of these Au-core/Ag-shell nanoparticles are 9.1, 11.4 and 23.2, respectively. Note that Au@(PAH-PAA)$_2$-1@Ag displays the highest SERS EF among all tested samples, indicating a very strong electromagnetic field. We thus attribute its slightly lower SEF EF to the quenching by Ag shell as there is no extra layer between the TBO molecules and the Ag shell. These results suggest that a strong, localized electromagnetic field is the main driving force behind both SERS and SEF. In addition, for SEF it is important to avoid or reduce the potential quenching by the metal via non-radiative loss. Both factors should be taken into consideration in order to achieve maximal SEF EFs.

In conclusion, we demonstrate a methodology to prepare Au-core/Ag-shell nanoparticles displaying both SEF and SERS activities simultaneously. Polyelectrolytes can be used to adjust the spacing and the dye position between the core and the shell. Layer-by-layer polyelectrolyte deposition can serve as an effective and flexible way to introduce various types of dye molecules into the nanostructures. The SEF enhancement appears to be more sensitive than the SERS enhancement to the position of the dye molecules. The results shed light to the intricacy between SEF and SERS. Such nanostructures should be useful for SEF and SERS based applications.

Supports from the US National Science Foundation (CBET-0931677, CBET-1065633) are gratefully acknowledged.

Notes and references

Department of Chemistry, University of Cincinnati, Cincinnati, OH 45221. Fax: 513-556-9239; Tel: 513-556-9222. E-mail: peng.zhang@uc.edu

† Electronic Supplementary Information (ESI) available: Experimental details. See DOI: 10.1039/b000000x/

1 (a) Fleischmann, M.; Hendra, P. J.; McQuillan, A. J. *Chem. Phys. Lett.* **1974**, *26*, 163; (b) Jeanmaire, D. L.; Van Duyne, R. P. *J. Electroanal. Chem.* **1977**, *84*, 1; (c) Moskovits, M. *J. Raman Spectrosc.* **2005**, *36*, 485; (d) Zhang, P.; Guo, Y. *J. Am. Chem. Soc.* **2009**, *131*, 3808.

2 (a) Chan, S.; Kwon, S.; Koo, T. W.; Lee, L. P.; Berlin, A. A. *Adv. Mater.* **2003**, *15*, 1595; (b) Doering, W. E.; Nie, S. *Anal. Chem.* **2003**, *75*, 6171.

3 Schatz, G. C.; Van Duyne, R. P. In *Handbook of Vibrational Spectroscopy*; Chalmers, J. M., Griffiths, P. R., Eds.; Wiley & Sons: **2002**.

4 (a) Aravind, P. K.; Metiu, H. *Surf. Sci.* **1983**, *124*, 506; (b) Liver, N.; Nitzan, A.; Gersten, J. I. *Chem. Phys. Lett.* **1984**, *111*, 449; (c) Kneipp, K.; Wang, Y.; Kneipp, H.; Perelman, L. T.; Itzkan, I.; Dasari, R. R.; Feld, M. S. *Phys. Rev. Lett.* **1997**, *78*, 1667; (d) Jiang, J.; Bosnick, K.; Maillard, M.; Brus, L. *J. Phys. Chem. B.* **2003**, *107*, 9964; (e) Aroca, R. F.; Goulet, P. J.; dos Santos, D. S. Jr.; Alvarez-Puebla, R. A.; Oliveira, O. N. Jr. *Anal. Chem.*, **2005**, *77*, 378; (f) Gandra, N.; Singamaneni. S. *Adv. Mater.* **2012**, *25*, 1022.

5 (a) Pinkhasova, P.; Puccio, B.; Chou, T.; Sukhishvili, S.; Du, H. *Chem. Commun.*, **2012**, *48*, 9750; (b) Li, W.; Guo, Y.; Zhang, P. *J. Phys. Chem. C.* **2010**, *114*, 7263.

6 (a) Aslan, K.; Lakowicz, J. R.; Geddes, C. D. *Anal. Bioanal. Chem.* **2005**, *382*, 926; (b) Lakowicz, J. R.; Ray, K.; Chowdhury, M.; Szmacinski, H.; Fu, Y.; Zhang, J.; Nowaczyk, K. *Analyst.* **2008**, *133*, 1308; (c) Hong, G. S.; Tabakman, S. M.; Welsher, K.; Wang, H. L.; Wang, X. R.; Dai, H. J. *J. Am. Chem. Soc.* **2010**, *132*, 1592.

7 (a) Lakowicz, J. R. *Anal. Biochem.* **2005**, *337*, 171; (b) Bardhan, R.; Grady, N. K.; Cole, J. R.; Joshi, A.; Halas, N. J. *ACS Nano.* **2009**, *3*, 744; (c) Wang, Y. K.; Yang, T. Y.; Tuominen, M. T.; Achermann, M. *Phys. Rev. Lett.* **2009**, *102*, 163001; (d) Muskens, O. L.; Giannini, V.; Sanchez-Gil, J. A.; Rivas, J. G. *Nano Lett.* **2007**, *7*, 2871.

8 (a) Gersten, J.; Nitzan, A. *J. Chem. Phys.* **1981**, *75*, 1139; (b) Wokaun, A.; Lutz, H. P.; King, A. P.; Wild, U. P.; Ernst, R. R. *J. Chem. Phys.* **1983**, *79*, 509.

Physical Chemistry Chemical Physics Accepted Manuscript

9 (a) Anger, P.; Bharadwaj, P.; Novotny, L. *Phys. Rev. Lett*. **2006**, *96*, 113002; (b) Guerrero, A. R. and Aroca, R. F. *Angew. Chem. Int. Ed*. **2011**, *50*, 665; (c) Gillz, R. and Le Ru, E. C. *Phys. Chem. Chem. Phys*. **2011**, *13*, 16366.

10 Li, J. F.; Huang, Y. F.; Ding, Y.; Yang, Z. L.; Li, S. B.; Zhou, X. S.; Fan, F. R.; Zhang, W.; Zhou, Z. Y.; Wu, D. Y.; Ren, B.; Wang, Z. L.; Tian, Z. Q. *Nature* **2010**, *464*, 392.

11 (a) Kim, K; Lee, Y. M.; Lee, H. B.; Shin, K. S. *ACS Appl. Mater. Interfaces*, **2009**, *1*, 2174; (b) Gabudean, A. M.; Biro, D; Astilean, S. *Nanotechnology.* **2011**, *23***,** 485706; (c) Kim, K; Lee, J. W.; Shin, K. S. *ACS Appl. Mater. Interfaces*. **2012**, *4*, 5498; (d) Gabudean, A. M.; Focsan, M; Astilean, S. *J. Phys. Chem. C*. **2012**, *116*, 12240; (e) Liu, Y; Wu, P. *ACS Appl. Mater. Interfaces.* **2013**, *5*, 5832.

12 Zhou, Y; Lee, C; Zhang, J; Zhang, P. *J. Mater. Chem. C*, **2013**, *1*, 3695.

13 Frens, G. *Nat. Phys. Sci.* **1973**, *241*, 20.

14 (a) Le Ru, E. C.; Etchegoin, P. G.; Grand, J.; Felidj, N.; Aubard J.; Levi, G. *J. Phys. Chem. C*. **2007**, *111*, 16076; (b) Klimov, V. V. and Guzatov, D. V. *Quantum Electron*. **2007**, *37*, 209.

Physical Chemistry Chemical Physics Accepted Manuscript

This journal is © The Royal Society of Chemistry [year]